engineering proceedings

In Vitro Antimicrobial and anticancer activity of metallic nanoparticles (Ag and and FeO) against Human pathogenic bacteria and cancer cell lines

Shama Parveen[1], Vikas Gupta[2*], Anuj knadawal[3] and Veera Nagendra Kumar[4]

[1]Department of Chemistry, Faculty of Science, Motherhood University, District- Haridwar, 247661 Uttarakhand (India).
2*Department of Chemistry, Faculty of Science, Motherhood University, District- Haridwar, 247661 Uttarakhand (India).
[2]Department of Chemistry, Faculty of Science, Harsh Vidya Mandir P.G.College, Raisi, District- Haridwar, 247661 Uttrakhand (India)
[3]Department of zoology, Faculty of Science, Government College for Men (Autonomous), Kadapa-516004, (India)
[4]Department of zoology, faculty of science, Government college for Men (autonomous), Kadapa-516004, (India)
* Correspondence: Corresponding author- polyiftm1@gmail.com

† Presented at The 4th International Electronic Conference on Applied Sciences, 27 October–10 November 2023.

Abstract

The global health community is extremely concerned about the emergence and spread of antibiotic resistance as well as the evolution of new strains of disease-causing organisms. It takes the creation of novel pharmaceuticals or access to a supply of innovative therapeutics for a disease to be effectively treated. Commonly used medicinal herbs in our society could be a great source of medications to combat this issue. The antibacterial and anticancer capabilities of the metallic nanoparticles made from plants are the main focus of this work. Two distinct nanoparticles were tested for their antibacterial and anticancer properties against four cancerous cell lines (Prostate cancer, lungs A549, HeLa and MCF-7) and five pathogenic microbes (Staphylococcus aureus, Bacillus subtilis, Pseudomons aeruginosa and Escherichia coli) bacteria, as well as one yeast (Candida albicans). Mettallic nanoparticles from the plants *Leucas cephalotes* (AgNPs) and *Ajuga macrosperma* (FeONPs) were tested for their antibacterial capabilities using the agar-well diffusion method and their ability to fight cancer using the MTS and MTT assays. According to the findings, AgNPs synthesized from *Leucas Cephalotes* showed the strongest potential against Pseudomons aeruginosa and Staphylococcus aureus. The zone of inhibition (ZOI) of *Leucas cephalotes's* AgNPs was 19 mm and 18 mm respectively, It was discovered also that the FeONPs of *Ajuga macrosperma* were found to have the most potential against the MCF-7 cancer cell line. Prostate cancer and lung cancer (A549) cell lines were the ones that responded most favourably to the AgNPs of *Leucas cephalotes*.

Keyword; antimicrobial activity, anticancer cancer activity, silver nanoparticles, iron oxide nanoparticles

1. Introduction

Antibiotics are essential for managing infectious disorders and preventing infection during difficult surgeries such organ transplants, joint replacements, or heart surgeries. However, it is evident that overusing antibiotics starts the emergence of microbial resistance [1]. The length of hospital stays increases as a result of multidru resistance to common infections, and fatality rates are also observed to rise. The need to research novel approaches to treating resistant bacteria results from this [2]. Cancer, which results in unchecked cell transformation, dynamic genome alteration, and the develop-

ment of malignant characteristics in normal cells, was also found to promote resistance to chemotherapy, a frequent cancer treatment [3]. The difficulties encountered in cancer therapy nowadays lead to limitations in the management of cancer, among them are the absence of an early diagnosis, nonspecific systemic distribution, insufficient drug concentrations reaching the tumour, and an inability to track therapeutic outcomes. medication delivery issues and medication retention at the target location are the root of serious consequences including multidrug resistance [3-4]. Technology may be able to provide answers to these existing cancer therapy roadblocks as well as to the problem of bacterial antibiotic resistance [5-6]. To be called "nanosized," a nanoparticle's size must fall between 1 and 100 nm [7]. Nanoscale is a field of science to the molecular scale regulation of substance. A material's chemical and physical characteristics change depending on its nanosize, ranging from those of larger substances or larger components. attention among scientist because of its extensive variety of applications.

Biological techniques for synthesizing NPs using plant leaf extracts or organisms like fungi, bacteria, and algae are considered eco-friendly substitutes for chemical synthesis because such approaches are nontoxic and less cost- and energy-intensive [8]. Plant extract-based NP production approaches are more beneficial than environmentally friendly biological approaches because cell cultures are not required [9]. Moreover, NPs production using plants is beneficial because of safe handling and easy availability associated with plants and their extensive metabolite content to facilitating reduction [10].

The main contributors to this phenomenon are a high surface area compared per unit volume ratio, surface plasmon resonance (SPAR), intense reactivity to chemicals, stability, high catalytic efficiency, remarkable strength in mechanics, and decreased melting temperatures [11]. Metal salts can be reduced in a solution or atoms can be gathered together to create metal nanoparticles.

2. Materials and methods

2.1. Chemicals and biological materials

Materials.

Leaves of Leucas cephalotes, and Ajuga macrosperma, Silver nitrate (AgNO3), copper sulphate, ferric sulphate, sodium hydroxide, distilled water. PC-3 (Prostate Cancer), Hela, A549 lung Cancer and MCF-7 (Breast Cancer) cell lines. Gram positive (Staphylococcus aureus and Bacillus subtilis) and Gram negative (Psreudomons aeruginosa and Escherichia coli) bacteria, as well as one yeast (Candida albicans) bacterial strain.

2.2. Collection of plants:

The leaves of the *Leucas cephalotes*, and *Ajuga macrosperma* obtained from the local forest in Kotdwara, Pauri Garhwal, India (June and September 2020).

2.3. Preparation of the Plant

Extract. After being dusted off with tap water, the gathered leaves of Leucas cephalotes, and Ajuga macrosperma were then rinsed with distilled water. A 500 ml and 1000 ml beaker containing 5g and 7g of leaves was combined with 150 ml, 300 ml, and 500 ml of sterile water that had been distilled. The combination was then heated for 120 minutes and allowed to cool to room temperature (30°C). The prepared mixture was coarsely ground in an Indian Ken Star kitchen blender before being filtered with Whatman filter paper No. 1. The filtrate was used to create iron oxide and silver nanoparticles.

2.4. Synthesis of nanoprticles

2.4.1. Synthesis of silver nanoparticles

The production of Ag-NPs required mixing the leaf extract with 60 ml of a 0.1 M solution of water of AgNO3 and stirring the mixture for 60 minutes at 60 °C. The tint changed after being mixed with the reduction mixture from brown to a dark brown col-

our was seen. After one hour, with reference to control, which indicates the confirmation was done by UV. Visible spectroscopy.

2.4.2. Synthesis of iron oxide nanoparticles

These nanoparticles of iron oxide were produced by combining one gramme of ferric sulphate with 50 milliliters of water that has been deionized and stirring the mixture at 80 °C for fifteen minutes. After being heated on the magnetic stirrer for two hours, the mixture of 50 ml of the FeSO4 mixture and 12 ml of the *Ajuga macrosperma* leaf extract. The NPs liquid's new coloration was a reddish brown at the same temperature.

2.5. Characterization

2.5.1. Characterization of silver and iron oxide nanoparticles.

The absorbance of pure NPs was measured using an ultraviolet (UV)-visible spectrophotometer (Bio-spectrophotometer BL 198, ELICO Ltd., India) in order to initially confirm the formation of NPs. NPs shape were determined using a scanningelectron microscope (JEOL2100F). X-ray diffraction was used to investigate the nanoparticles' crystal structure. X-ray diffractometers with Cu-K radiations in the 2° range of 5° to 80° (Bruker Nano D8 ADVANCE, GmbH, Germany) were used to obtain the X-ray diffraction (XRD) pattern. The zeta potential of NPs (Malvern, Malvern Instruments Ltd., UK) was measured in the range of -200 mV to 200 mV at 25°C, using a count rate of 189.8 Kcps, to determine the stability of the system. Fourier-transform Infrared spectrophotometer (Microscope with Vertex 80 FTIR System, Bruker, Germany) was used for the analysis, which covered the wavelength range from 4,000 to 400 cm1.

2.6. Antimicrobial Activity

2.6.1. Method

E. coli, Staphylococcus aureus, Bacillus subtilis, Pseudomonas aeruginosa, and Candida albicans were the MDR clinical isolates that were inoculated into Mueller Hinton broth. The culture was kept at 37°C until the absorbance at 600 nm reached 0.8 O.D. (8 McFarland's standard). To assess the antibacterial potential of AgNPs and FeONPs, the agar well diffusion method was used with various modifications. Molten soft agar was mixed with one milliliter of 0.5 McFarland inoculum, then the mixture was put onto basal agar plates and allowed to set. With the aid of a cork borer, 6mm wells in soft agar were bored, and 20 l of hour were added. The wells were then incubated at 37°C for 24 hours. We measured the zone of inhibition. [table 1].

2.6.2. Cell Cytotoxicity

The PC3, A549 human lung cancer cell line, MCF-7, and HeLa with slight modification have been employed for the studies on cell cytotoxicity. The MTT and MTS (3-(4,5-dimethylthiazol-2-yl)-5-(3-carboxymethoxyphenyl)-2-(4-sulphonyl)-2H-tetrazolium) assays were applied to determine the state of health of the cells. Succinate dehydrogenase enzymes reduced MTT in the mitochondria of metabolically active cells, producing reducing equivalents like NADH and NADPH. The crystal of purple formazan that is insoluble was created. A spectrophotometer was used to measure the crystal after it had been solubilized in DMSO. In 96-well culture plates, 5,000 A549 cells per well were seeded and cultured for 24 hours in RPMI-1640 culture media. After being seeded for 24 hours, the cells were exposed to AgNP, CuONPs, and FeONPs that had been biologically produced at concentrations of 100, 200, 400, 600, and 800 g/ml for 48 hours, with 50 M fisetin serving as a positive control. Fresh 100 l of 5 mg/ml of MTT solution was introduced to each well after 48 hours, and each well was subsequently incubated for three to four hours at 37°C in a CO2 incubator. The 100 l of DMSO was added after the MTT solution had been taken out. For the disintegration of the formazan crystals, the solution was left in the sterilizer for 15 minutes.

Thermo Scientific's Varioskan Flash microplate reader was used to read the plates at 570 nm following a brief premixing step. The method used to determine the percentage of viable cells is as follows: percentage of viable cells = average absorbance by treatment sample/average absorbance by control sample multiplied by 100.

3. Result and Discussion

In the present study, plant -mediated silver and iron oxide nanoparticles were explored by using silver nitrate and ferric sulphate as a reducing agent. The reaction mixture turned from colorless to brown and dark brown, which is the preliminary indication of the synthesis of AgNPs and FeONPs. It was confirmed by Uv analysis.

3.1. Spectra of AgNPs and FeONP.

3.1.1. UV-Visible

The technique of ultraviolet-visible spectroscopy is often employed to describe nanoparticles. The recognizable absorption in the visible range is caused by the metallic nanoparticles' surface plasmon resonance. Utilizing the 200–800 nm UV–visible spectrum, the absorbed energy of NPs was calculated. The absorbance at 432, and 218 nm, which is specific to silver, and iron oxide nanoparticles was observed, as can be seen in Figure 1(a) and related to previous literature [12,13]. In an aqueous solution, silver and iron oxide nanoparticles have a brownish-yellow and red hue.

3.1.2. XRD

The diffraction intensities ranged between 20 to 80, and strong Bragg reflections were observed at 38.45, 44.28, 64.20, and 78.08, respectively, which is indexable by the facets of AgNPs' fcc crystalline makeup, and which correspond to the planes of (111), (200), (220), and (311) [14]. It was discovered that the usual AgNP pattern produced by green syntheses has a fcc structure. The miller indices were found at (101), (221), and (200), coupled with the diffraction peaks at 11.62, 16.49, and 31.28. The standard data (JPCDS-01-079-1973) match with synthesized FeoNPs data. These data indicates that these diffraction spikes point to a body centre cubic (BBC) configuration. [15]. Using Debye Scherrer' equation, was possible to evaluate the silver an iron oxide nanoparticles' typical particles size. The crytalline average size of AgNPs and FeONPs was 24 and 37 nm. .

3.1.3. FTIR

Biogenic synthesis of silver and iron oxide nanoparticles utilizes the plant extract as the reducing and capping agent. The FTIR analysis reveals groups involved in the reducing and capping agent, that is, groups preventing aggregation of silver and iron oxide nanoparticles. By comparing FTIR (Figure 2a and 2b) of AgNPs and FeONPs. The FT-IR spectra of AgNPs made by *Leucas cephalotes* leaf extract shows. The FTIR spectra showed numerous distinct bands about 3736, 2308, 1691, 1556, 902, 682, and 418 cm^{1}. The hydroxyl (O-H) functional group of polyphenolic species has a stretching vibration that has an absorption peak at 3736.12 cm^{1}. The peaks at 1691 and 2308 cm-1 are probably the result of the carbonyl (C=O) vibratory stretching originating from highly conjugated systems. In accordance with the Ag nanoparticles, peak at 682 and 410 is located. The FTIR spectra for synthesized iron oxide nanoparticles revealed multiple distinct bands, at 3738.05 cm-1 and 3633.89 cm-1 show stretching vibrations of the -O-H functional group. The peak in absorption at 2306 cm-1 indicates the presence of the functional group (C-O). The signal detected at 1687 cm-1 may be due to carbonyl (C=O) stretching vibrations generated by highly conjugated systems. The prominence at 1068 cm-1 might serve as a representation of the (C-H) functional group.

3.2. Zeta Potential.

The zeta potential is determined in order to explore the solution's colloidal stability. The term "zeta potential" refers to the electric potential of the particles at the double layer's interface. The microscopic particles are stable due to the surface charge covering them, which also inhibits agglomeration. According to Figure 4(a, b, and c), NPs have a zeta potential of -23.36, and -27.06 mV, correspondingly. This reading demonstrates the NPs' stability.

3.3. Morphology

3.3.1. SEM with EDX

Using the electron micrograph of the complex as a starting point, the SEM may examine the skeletal anatomy of the synthesised AgNPs and FeONPs. The NPs' predominate shape was demonstrated to be spherical and cubic. According to the study, SEM photos demonstrate the spherical shape and size of the AgNPs produced by Leucas cehalotes, which are in the a wavelength ranging from 10 to- 100 nm range.[16] A similar outcome for AgNPs was reported according to Figure 6.54 (a), which depicts a 2 m with a magnification of 20 KX using picture 6.54 (b), which depicts the 1 m with 25.000 KX magnification. Imaging at higher magnifications is done using FESEM. As indicated in the figure (4a, 4b) iron oxide nanoparticles made with *Ajuga macrosperma* leaf extract have a cube form and a selection of sizes of 5-27 nm. Similar results have previously been reported [17].

EDAX analysis, which validates the presence of silver and iron as a significant metallic element establishes the existence of metallic iron nanoparticles. The presence of silver, iron and oxide was identified using the EDX spectrum. Using EDX, the weight percentages silver (48.93%) of iron (51.02%), oxide (39.14%), and other elements (3.14%) were calculated

3.4. Antimicrobial Activity

The biogenic silver and iron oxide nanoparticles acquired from the aqueous leaf extracts of *Leucas cephalotes* and *Ajuga macrosperma* were investigated for antimicrobial potential against MDR clinical bacterial isolates by utilizing the agar well diffusion method. The MDR clinical isolates of E. coli, Shigella spp., Pseudomonas aeruginosa, Aeromonas spp., and Candida tropicalis were susceptible to NPs. From Table 1, it shows that Pseudomonas aeruginosa was more sensitive than staphylococs auresus, Thus, AgNP which is create by *Leucas cephalotes* plant extract are effective on yeast Candida albians. Strangely, stand-alone FeONPs (created by macrosperma) did not show antimicrobial activity.

According to antibacterial effectiveness against gram-positive bacteria and gram negative bacteria, the inhibition zone's variation is recorded. Table 1 shows the values of the inhibitory zones for staphylococcus aureus **Pseudomons aeruginosa, candida albians. Escherichia coli.** and Bacillus subtilis for both NPs which were produced by combining the leaf extracts of *Leucas Cephalotes* and *Ajuga macrosperma* moreover.

3.4.1. Antimicrobial activity of Silver nanoparticles towards gram postive, gram negative and yeast

Regarding the antibacterial action, the inhibition zone's variation is observed when it comes to gram-positive bacteria. Table 1 shows the values of the inhibitory zones for staphylococcus aureus and Bacillus subtilis for AgNPs, which were made from the leaf extracts of *Leucas Cephalotes,* Additionally, it was found that the silver nanoparticles had extremely high activity against staphylococcus aureus, Pseudomons aeruginosa and candida albians. However, AgNPS show less activity towards Bacillus Subtilis and Escherichia coli.

3.4.2. Antimicrobial activity of iron oxide nanoparticles towards Gram postive and gram negative and yeast

Regarding the antibacterial action, varying inhibition zone is reported against gram-positive bacteria. FeONPs were created by the leaf extracts of *Ajuga macrosprerma* the values of the inhibitory zones for staphylococcus aureus, Pesudomonas aeruginosa. E. coli. Candida albian and Bacillus subtilis are shown in table 2. Additionally, it was found that FeONPs showed high activity against Pesudomonas aeruginosa and E. coli and no activity shows towards Bacillus subtilis and candida albians.

Recently, Ludwigia octovalvis [18], Solanum nigrum leaves [19], Mimusops elengi fruit [20] Salacia chinensis L [21] Vitex negundo [22] Mimusops elengi, Linn. [23] Laurus nobilis [24] extract mediated synthesized Ag NPs was reported the antibacterial activity against the gram negative and gram positive stain [25-26].

Table 1. Shows the inhibition zones for nanoparticles of silverand iron oxide produced using the Agar well diffusion method.

S.N.	Sample name	Bacteria name	Zone of inhibition
1.	AgNPs	S. aureu	18
		B. Subtilis	12
		E. coli	12
		P. aeruginosa	19
		Candida albicans	16
2.	ZnONPs	S. aureu	17
		B. Subtilis	NI
		E. coli	12
		P. aeruginosa	NI
		Candida albicans	NI

3.5. Anticancer activity

The synthesized AgNPs and FeONPs were determined the anticancer (cytotoxicity) activity in the prostate , lungs and human breast cancer cells using MTT and MTS assay. MDA-MB-231 human breast cancer cells were also treated with different concentrations (100, 33.33, 11.11, 3.70, 1.23 and 0.41μg/mL) of synthesized AgNPs and FeONPs. After, 24 h the treated cells were examined the changes of nuclear morphology (Fig. 7(a–f)). The cells viability was considerably reduced in the presence of green synthesized AgNPs anf FeONPs as compared with the positive/negative control. At 24 h treatment, the IC50 value of the AgNPs was found to be **± 2.11, ± 2.01 and ± 3.21**μg/mL for prostate (PC-3),

lungs (A-549) and human breast (HeLa) cancer. And FeONPs was observed **± 2.65, 8.90 and 4.65 µg/**mL respectively. These result shows that the minimum dose of synthesized Ag NPs and FeONPs showed good cytotoxicity activity against the prostate (PC-3), lungs (A-549) and human breast (HeLa) cancer cell lines (shown in table2). AgNPs had highest cytotoxicity activity towards lungs cancer cell lines among other cancer cell lines. Additionaly it was aslo studied that synthesiszed AgNPs and FeONPs were determined the anticancer (cytotoxicity) activity in the human breast cancer (MCF-7) cells using MTT assay. The results shows that minimum dose of FeONPs shows excellent activity towards MCF-7 cancer cell lines. Several studies suggest that the remarkable cytotoxicity (anticancer) of biologically synthesized MNPs was increased with the increasing concentration of NPs [27, 28, 29].

Table 2. show the IC50 of synthesized metallic nanoparticles against MCF-7(breast cancer), HeLa, PC-3 (prostate cancer), A549 (Lungs cancer) cell lines.

S.N.	Plant name	Nanoparticles name	PC-3 (Prostate Cancer) IC_{50}	Hela IC_{50}	A549 (lung Cancer) IC_{50}	MCF-7 (Breast Cancer) IC_{50}
1.	Abides Pindrow royle	FeONPs	1.23	2.0	3.98	1.91
2.	Ajuga macrosperma	FeONPs	2.65	4.78	8.97	1.10

3.6. Conclusion

We have synthesized the silver and iron oxide nanoparticles using aqueous Leaf extract of *Leucas cephalotes* and *Ajuga macrosperma* in a rapid, straightforward, economical and environment-friendly manner without involvement of hazardous chemicals. Various reaction parameters such as concentration of extract and AgNO3 and FeSO4 solution, pH and reaction time and temperature were optimized for synthesis of AgNPs and FeONPs. The NPs were spherical and cubic in shape with particle size 10 to 30 nm and negative zeta potential of -23.36, and -27.06 mV.

The NPs were stable over a period of 10 d at room temperature and demonstrated antimicrobial and anticancer property. The biosynthesized AgNPs and FeONPs showed in vitro anticancer activity in breast (MCF-7 and HeLa), prostate cancer (PC-3), Lungs (A-549) cancer cell lines. The biosynthesizes AgNPs and FeONPs showed also good antimicrobal activity against five pathogenic microbes (Staphylococcus aureus, Bacillus subtilis, Pseudomons aeruginosa and Escherichia coli). The AgNPs could be further explored as therapeutic agents in the treatment of cancer.

Figures

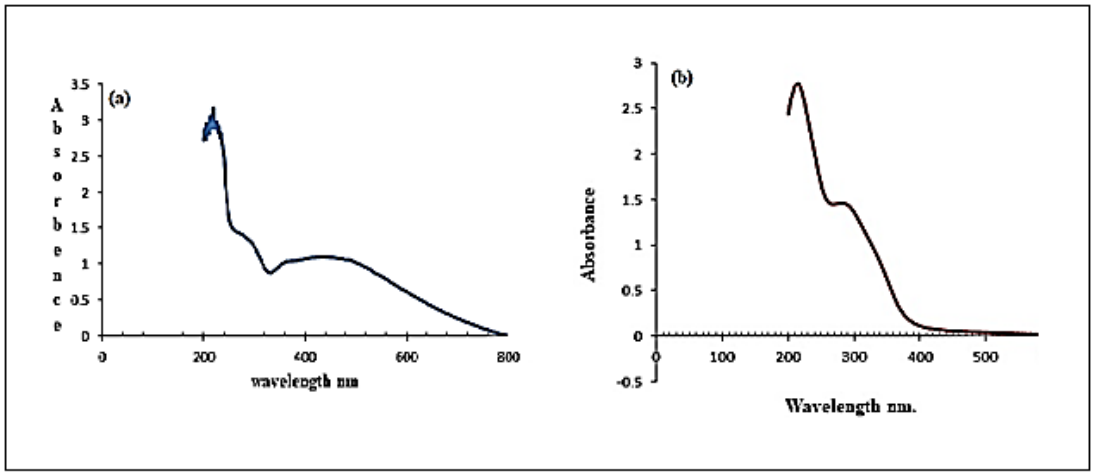

Figure 1. UV. Visible spectra (a) AgNPs spectra using *Leucas Cephalotes* leaf extract. (b) FeONPs spectra using *Ajuga macrosperma* leaf exract.

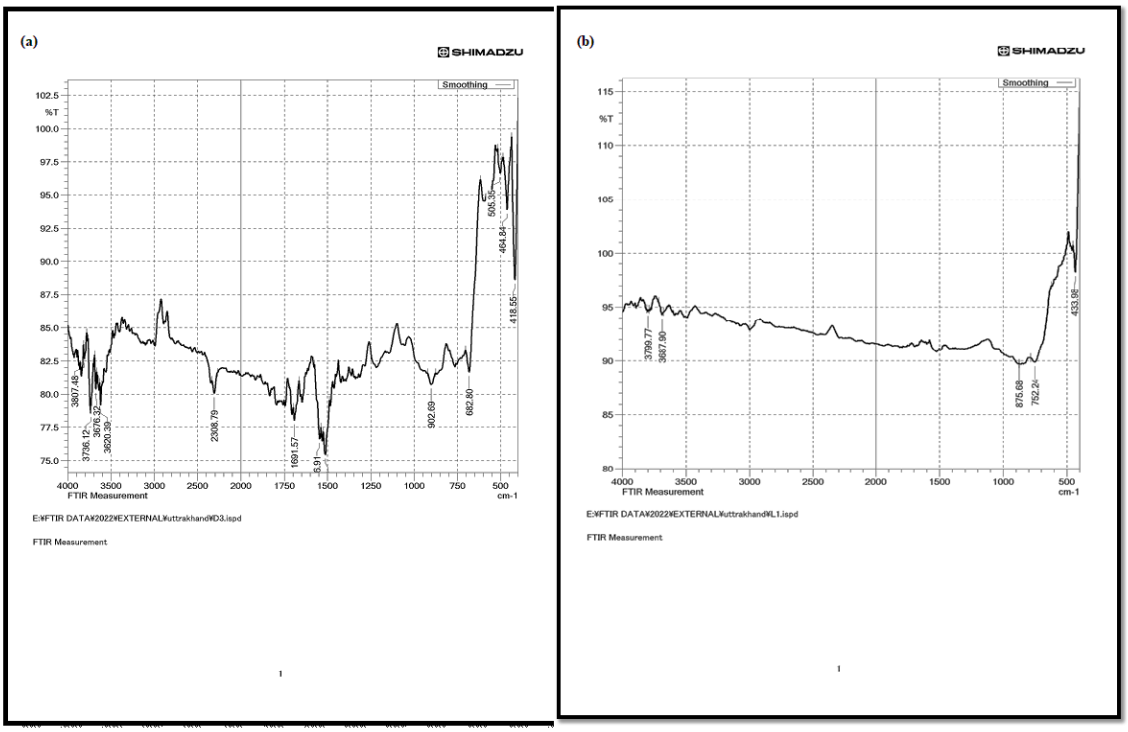

Figure 2. FTIR spectra (a) AgNPs spectra using *Leucas Cephalotes* leaf extract. (b) FeONPs spectra using *Ajuga macrosperma* leaf exract.

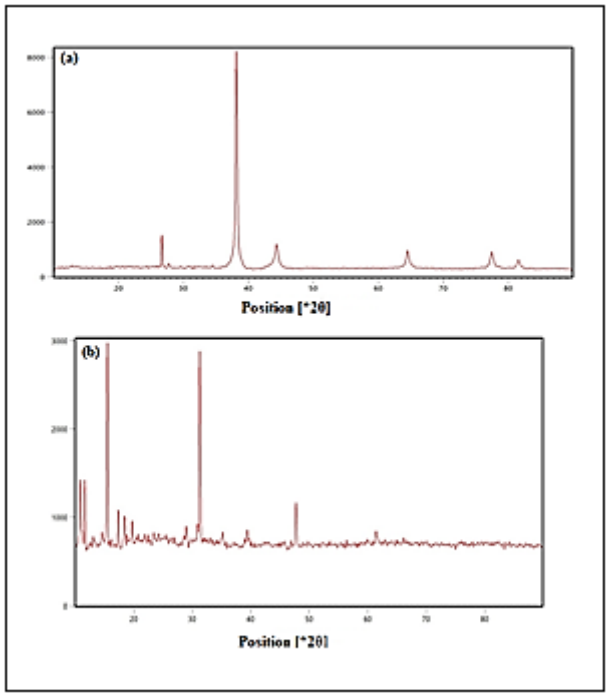

Figure 3. XRD spectra (a) AgNPs spectra using *Leucas Cephalotes* leaf extract. (b) FeONPs spectra using *Ajuga macrosperma* leaf exract.

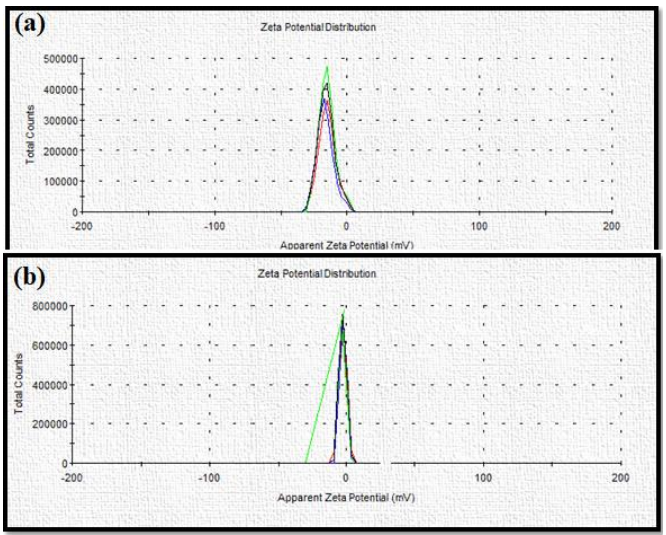

Figure 4. Morphology (a) SEM image of AgNPs (b) SEM image of FeONPs.

Fig. 5. Zeta potential of (a) AgNPs (b) FeONPs.

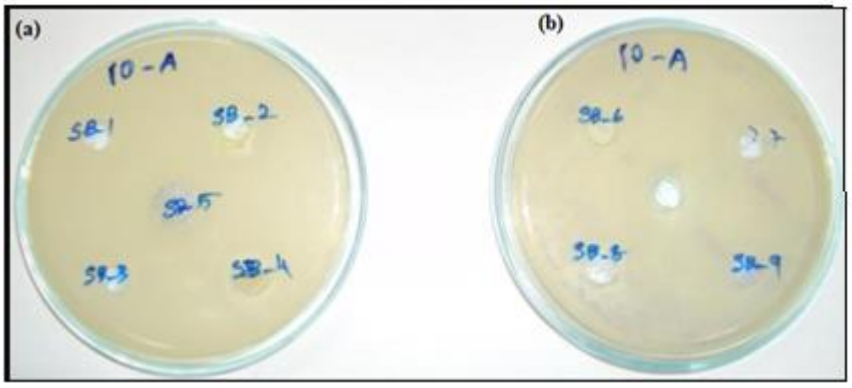

Figure 6. Antimcrobial activity of synthesized nanoparticles against Staphylococcus aureus, Bacillus subtilis, Pseudomons aeruginosa and Escherichia coli. (a) AgNPs (b) FeONPs.

References

1. Abalkhil TA, Alharbi SA, Salmen SH, Wainwright M. Bactericidal activity of biosynthesized silver nanoparticles against human pathogenic bacteria. Biotechnology & Biotechnological Equipment. 2017 Mar 4;31(2):411-7.

2. Munita JM, Arias CA. Mechanisms of antibiotic resistance. Virulence mechanisms of bacterial pathogens. 2016 Jun 22:481-51

3. Mansoori B, Mohammadi A, Davudian S, Shirjang S, Baradaran B. The different mechanisms of cancer drug resistance: a brief review. Advanced pharmaceutical bulletin. 2017 Sep;7(3):339.

4. Nile A, Nile SH, Shin J, Park G, Oh JW. Quercetin-3-glucoside extracted from apple pomace induces cell cycle arrest and apoptosis by increasing intracellular ROS levels. International Journal of Molecular Sciences. 2021 Oct 4;22(19):10749.

5. Siddiqi KS, Husen A, Rao RA. A review on biosynthesis of silver nanoparticles and their biocidal properties. Journal of nanobiotechnology. 2018 Dec;16(1):1-28.

6. Patel SK, Kalia VC. Advancements in the nanobiotechnological applications. Indian Journal of Microbiology. 2021 Dec 1:1-3.

7. Nakamura S, Sato M, Sato Y, Ando N, Takayama T, Fujita M, Ishihara M. Synthesis and application of silver nanoparticles (Ag NPs) for the prevention of infection in healthcare workers. International journal of molecular sciences. 2019 Jul 24;20(15):3620.

8. Hosseini-Koupaei M, Shareghi B, Saboury AA, Davar F, Sirotkin VA, Hosseini-Koupaei MH, Enteshari Z. Catalytic activity, structure and stability of proteinase K in the presence of biosynthesized CuO nanoparticles. International journal of biological macromolecules. 2019 Feb 1;122:732-44.

9. Tavakoli S, Kharaziha M, Ahmadi S. Green synthesis and morphology dependent antibacterial activity of copper oxide nanoparticles. Journal of Nanostructures. 2019 Jan 1;9(1):163-71.

10. Berra D, Laouini SE, Benhaoua B, Ouahrani MR, Berrani D, Rahal A. Green synthesis of copper oxide nanoparticles by Pheonix dactylifera L leaves extract. Digest Journal of Nanomaterials and Biostructures. 2018 Oct 1;13(4):1231-8.

11. Nile SH, Baskar V, Selvaraj D, Nile A, Xiao J, Kai G. Nanotechnologies in food science: applications, recent trends, and future perspectives. Nano-micro letters. 2020 Dec;12:1-34.

12. Díaz M, Barba F, Miranda M, Guitián F, Torrecillas R, Moya JS. Synthesis and antimicrobial activity of a silver-hydroxyapatite nanocomposite. Journal of Nanomaterials. 2009 Jan 1;2009:1-6.

13. Kumar KM, Mandal BK. Speciation of green iron nanoparticles in situ by a simple UV-Visible technique. Journal of the indian cdhemidcal society. 2012 Dec 1;89(12):1653-8.

14. //

15. Prakash P, Gnanaprakasam P, Emmanuel R, Arokiyaraj S, Saravanan M. Green synthesis of silver nanoparticles from leaf extract of Mimusops elengi, Linn. for enhanced antibacterial activity against multi drug resistant clinical isolates. Colloids and Surfaces B: Biointerfaces. 2013 Aug 1;108:255-9.

16. Abid MA, Kadhim DA, Aziz WJ. Iron oxide nanoparticle synthesis using trigonella and tomato extracts and their antibacterial activity. Materials Technology. 2022 Jul 3;37(8):547-54.

17. Sayed FN, Polshettiwar V. Facile and sustainable synthesis of shaped iron oxide nanoparticles: effect of iron precursor salts on the shapes of iron oxides. Scientific reports. 2015 May 5;5(1):9733.

18. Sarathi Kannan D, Mahboob S, Al-Ghanim KA, Venkatachalam P. Antibacterial, antibiofilm and photocatalytic activities of biogenic silver nanoparticles from Ludwigia octovalvis. Journal of Cluster Science. 2021 Mar;32:255-64.

19. Jenifer AA, Malaikozhundan B, Vijayakumar S, Anjugam M, Iswarya A, Vaseeharan B. Green synthesis and characterization of silver nanoparticles (AgNPs) using leaf extract of Solanum nigrum and assessment of toxicity in vertebrate and invertebrate aquatic animals. Journal of Cluster Science. 2020 Sep;31:989-1002.

20. Korkmaz N, Ceylan Y, Hamid A, Karadağ A, Bülbül AS, Aftab MN, Çevik Ö, Şen F. Biogenic silver nanoparticles synthesized via Mimusops elengi fruit extract, a study on antibiofilm, antibacterial, and anticancer activities. Journal of Drug Delivery Science and Technology. 2020 Oct 1;59:101864.

21. Nagesh MR, Kumar N, Khan JM, Ahmed MZ, Kavitha R, Kim SJ, Vijayakumar N. Green synthesis and pharmacological applications of silver nanoparticles using ethanolic extract of Salacia chinensis L. Journal of King Saud University-Science. 2022 Oct 1;34(7):102284.

22. Dogra S, Sharma MD, Tabassum S, Mishra P, Bhatt AK, Bhuyar P. GREEN BIOSYNTHESIS OF SILVER NANOPARTICLES (AgNPs) FROM Vitex negundo PLANT EXTRACT AND ITS PHYTOCHEMICAL SCREENING AND ANTIMICROBIAL ASSESSMENT NEXT TO PATHOGENIC MICROBES. Journal of Microbiology, Biotechnology & Food Sciences. 2023 Feb 1;12(4).

23. Prakash P, Gnanaprakasam P, Emmanuel R, Arokiyaraj S, Saravanan M. Green synthesis of silver nanoparticles from leaf extract of Mimusops elengi, Linn. for enhanced antibacterial activity against multi drug resistant clinical isolates. Colloids and Surfaces B: Biointerfaces. 2013 Aug 1;108:255-9.

24. Al-Ghamdi AY. Antimicrobial and catalytic activities of green synthesized silver nanoparticles using bay laurel (Laurus nobilis) leaves extract. Journal of Biomaterials and Nanobiotechnology. 2019 Jan 9;10(1):26-39.

25. Chandrasekar N, Kumar K, BALASUBRAMNIAN KS, Karunamurthy K, VARADHARAJAN R. FACILE SYNTHESIS OF IRON OXIDE, IRON-COBALT AND ZERO VALENT IRON NANOPARTICLES AND EVALUATION OF THEIR ANTI MICROBIAL ACTIVITY, FREE RADICLE SCAVENGINGING ACTIVITY AND ANTIOXIDANT ASSAY. Digest Journal of Nanomaterials & Biostructures (DJNB). 2013 Apr 1;8(2).

26. Krishnaraj C, Muthukumaran P, Ramachandran R, Balakumaran MD, Kalaichelvan PT. Acalypha indica Linn: biogenic synthesis of silver and gold nanoparticles and their cytotoxic effects against MDA-MB-231, human breast cancer cells. Biotechnology Reports. 2014 Dec 1;4:42-9.

27. Liu H, Shi W, Luo Y, Cui G, Kong X, Han L, Zhao L. Green supported of Au nanoparticles over reduced graphene oxide: Investigation of its cytotoxicity, antioxidant and anti-human breast cancer properties. Inorganic Chemistry Communications. 2021 Dec 1;134:108918.

28. Biresaw SS, Taneja P. Copper nanoparticles green synthesis and characterization as anticancer potential in breast cancer cells (MCF7) derived from Prunus nepalensis phytochemicals. Materials Today: Proceedings. 2022 Jan 1;49:3501-9.

29. Banerjee S, Islam S, Chattopadhyay A, Sen A, Kar P. Synthesis of silver nanoparticles using underutilized fruit Baccaurea ramiflora (Latka) juice and its biological and cytotoxic efficacy against MCF-7 and MDA-MB 231 cancer cell lines. South African Journal of Botany. 2022 Mar 1;145:228-35.